

# Momentum space topology and quantum phase transitions

G.E. Volovik

Low Temperature Laboratory, Helsinki University of Technology  
P.O.Box 2200, FIN-02015 HUT, Finland

L.D. Landau Institute for Theoretical Physics  
Kosygin Str. 2, 119334 Moscow, Russia

February 22, 2019

## Abstract

Many quantum condensed-matter systems, and probably the quantum vacuum of our Universe, are strongly correlated and strongly interacting fermionic systems, which cannot be treated perturbatively. However, physics which emerges in the low-energy does not depend on the complicated details of the system and is relatively simple. It is determined by the nodes in the fermionic spectrum, which are protected by topology in momentum space (in some cases, in combination with the vacuum symmetry). Here we illustrate this universality on some examples of quantum phase transitions, which can occur between the vacua with the same symmetry but with different topology in momentum space. The quantum phase transitions between the fully gapped states with different momentum-space topology are also discussed.

## 1 Introduction.

There are two schemes for the classification of states in condensed matter physics and relativistic quantum fields: classification by symmetry (GUT scheme) and by momentum space topology (anti-GUT scheme).

For the first classification method, a given state of the system is characterized by a symmetry group  $H$  which is a subgroup of the symmetry group  $G$  of the relevant physical laws. The thermodynamic phase transition between equilibrium states is usually marked by a change of the symmetry group  $H$ . This classification reflects the phenomenon of spontaneously broken symmetry. In relativistic quantum fields the chain of successive phase transitions, in which the large symmetry group existing at high energy is reduced at low energy, is in the basis of the Grand Unification models (GUT) [1, 2]. In condensed matter the spontaneous symmetry breaking is a typical phenomenon, and the thermodynamic states are also classified in terms of the subgroup  $H$  of the relevant group  $G$  (see e.g. the classification of superfluid and superconducting states in Refs. [3, 4]). The groups  $G$  and  $H$  are also responsible for topological defects, which are determined by the nontrivial elements of the homotopy groups  $\pi_n(G/H)$ ; cf. Ref. [5].

The second classification method reflects the opposite tendency – the anti Grand Unification (anti-GUT) – when instead of the symmetry breaking the symmetry gradually emerges at low energy. This method deals with the ground states of the system at zero temperature ( $T = 0$ ), i.e., it is the classification of quantum vacua. The universality classes of quantum vacua are determined by momentum-space topology, which is also responsible for the type of the emergent physical laws at low energy.

For systems living in 3D space, there are four basic universality classes of fermionic vacua [6, 7]:

- (i) Vacua with fully-gapped fermionic excitations, such as semiconductors and conventional superconductors.
- (ii) Vacua with fermionic excitations characterized by Fermi points – points in 3D momentum space at which the energy of fermionic quasiparticle vanishes. Examples are provided by superfluid  $^3\text{He-A}$  and also by the quantum vacuum of Standard Model above the electroweak transition, where all elementary particles are Weyl fermions with Fermi points in the spectrum. This universality class manifests the phenomenon of emergent relativistic quantum fields at low energy: close to the Fermi points the fermionic quasiparticles behave as massless Weyl fermions, while the collective modes of the vacuum interact with these fermions as gauge and gravitational fields.
- (iii) Vacua with fermionic excitations characterized by lines in 3D momentum space or points in 2D momentum space. We call them Fermi lines, though in general it is better to characterize zeroes by co-dimension, which

is the dimension of  $\mathbf{p}$ -space minus the dimension of the manifold of zeros. Lines in 3D momentum space and points in 2D momentum space have co-dimension 2: since  $3 - 1 = 2 - 0 = 2$ ; compare this with zeroes of class (ii) which have co-dimension  $3 - 0 = 3$ . The Fermi lines are topologically stable only if some special symmetry is obeyed. Example is provided by the vacuum of the high  $T_c$  superconductors where the Cooper pairing into a  $d$ -wave state occurs. The nodal lines (or actually the point nodes in these effectively 2D systems) are stabilized by the combined effect of momentum-space topology and time reversal symmetry.

(iv) Vacua with fermionic excitations characterized by Fermi surfaces. The representatives of this universality class are normal metals and normal liquid  $^3\text{He}$ . This universality class also manifests the phenomenon of emergent physics, though non-relativistic: at low temperature all the metals behave in a similar way, and this behavior is determined by the Landau theory of Fermi liquid which is based on the existence of Fermi surface. Fermi surface has co-dimension 1: in 3D system it is the surface (co-dimension  $= 3 - 2 = 1$ ), in 2D system it is the line (co-dimension  $= 2 - 1 = 1$ ), and in 1D system it is the point (co-dimension  $= 1 - 0 = 1$ ; in one dimensional system the Landau Fermi-liquid theory does not work, but the Fermi surface survives).

The possibility of the Fermi band class (v), where the energy vanishes in the finite region of the 3D momentum space and thus zeroes have co-dimension 0, has been also discussed [8, 9]. This is still not well established, the latest references can be found in [10, 11].

The phase transitions which follow from this classification scheme are quantum phase transitions which occur at  $T = 0$  [12]. It may happen that by changing some parameter  $q$  of the system we transfer the vacuum state from one universality class to another, or to the vacuum of the same universality class but different topological quantum number, without changing its symmetry group  $H$ . The point  $q_c$ , where this zero-temperature transition occurs, marks the quantum phase transition. For  $T \neq 0$ , the second order phase transition is absent, as the two states belong to the same symmetry class  $H$ , but the first order phase transition is not excluded. Hence, there is an isolated singular point  $(q_c, 0)$  in the  $(q, T)$  plane (see Fig. 1), or the end point of the first order transition.

The quantum phase transitions which occur in classes (iv) and (i) or between these classes are well known. In the class (iv) the corresponding

quantum phase transition is known as Lifshitz transition [13], at which the Fermi surface changes its topology or emerges from the fully gapped state of class (i), see Sec. 2.2. The transition between the fully gapped states characterized by different topological charges occurs in 2D systems exhibiting the quantum Hall and spin-Hall effect: this is the plateau-plateau transition between the states with different values of the Hall (or spin-Hall) conductance (see Sec. 5). The less known transitions involve nodes of co-dimension 3 [14, 15, 16, 17, 18] (Sec. 3 on Fermi points) and nodes of co-dimension 2 [19, 20, 21, 23] (Sec. 4 on nodal lines).

## 2 Fermi surface and Lifshitz transition

### 2.1 Fermi surface as topological object

In ideal Fermi gases, the Fermi surface at  $p = p_F = \sqrt{2\mu m}$  is the boundary in  $\mathbf{p}$ -space between the occupied states ( $n_{\mathbf{p}} = 1$ ) at  $p^2/2m < \mu$  and empty states ( $n_{\mathbf{p}} = 0$ ) at  $p^2/2m > \mu$ . At this boundary (the surface in 3D momentum space) the energy is zero. What happens when the interaction between particles is introduced? Due to interaction the distribution function  $n_{\mathbf{p}}$  of particles in the ground state is no longer exactly 1 or 0. However, it appears that the Fermi surface survives as the singularity in  $n_{\mathbf{p}}$ . Such stability of the Fermi surface comes from a topological property of the one-particle Green's function at imaginary frequency:

$$G^{-1} = i\omega - \frac{p^2}{2m} + \mu . \quad (1)$$

Let us for simplicity skip one spatial dimension  $p_z$  so that the Fermi surface becomes the line in 2D momentum space  $(p_x, p_y)$ ; this does not change the co-dimension of zeroes which remains  $1 = 3 - 2 = 2 - 1$ . The Green's function has singularities lying on a closed line  $\omega = 0$ ,  $p_x^2 + p_y^2 = p_F^2$  in the 3D momentum-frequency space  $(\omega, p_x, p_y)$  (see Fig. 2). This is the line of the quantized vortex in the momentum space, since the phase  $\Phi$  of the Green's function  $G = |G|e^{i\Phi}$  changes by  $2\pi N_1$  around the path embracing any element of this vortex line. In the considered case the phase winding number is  $N_1 = 1$ . If we add the third momentum dimension  $p_z$  the vortex line becomes the surface in the 4D momentum-frequency space  $(\omega, p_x, p_y, p_z)$

– the Fermi surface – but again the phase changes by  $2\pi$  along any closed loop embracing the element of the 2D surface in the 4D momentum-frequency space.

The winding number cannot change by continuous deformation of the Green's function: the momentum-space vortex is robust toward any perturbation. Thus the singularity of the Green function on the Fermi surface are preserved, even when interaction between fermions is introduced. The invariant is the same for any space dimension, since the co-dimension remains 1.

The Green function is generally a matrix with spin indices. In addition, it may have the band indices (in the case of electrons in the periodic potential of crystals). In such a case the phase of the Green function becomes meaningless; however, the topological property of the Green function remains robust. But now the winding number  $N_1$ , which is responsible for the stability of the Fermi surface, is written in the general matrix form

$$N_1 = \text{tr} \oint_C \frac{dl}{2\pi i} G(\mu, \mathbf{p}) \partial_l G^{-1}(\mu, \mathbf{p}) . \quad (2)$$

Here the integral is taken over an arbitrary contour  $C$  around the momentum-space vortex, and  $\text{tr}$  is the trace over the spin, band or other indices.

## 2.2 Lifshitz transition

There are two scenarios of how to destroy the vortex loop in momentum space: perturbative and non-perturbative. In the second scenario the non-perturbative reconstruction of the spectrum removes the Fermi surface, as it occurs at the superconducting transition when the gap appears.

In the perturbative case the Fermi surface cannot be destroyed since it is protected by topology and thus is robust to perturbations. The Fermi surface can be removed in the process which reproduces the process occurring for the real-space counterpart of the Fermi surface – the loop of quantized vortex in superfluids and superconductors. The vortex ring can continuously shrink to a point and then disappear. This is allowed by topology, since the opposite elements of the vortex line have opposite winding numbers, which annihilate each other:  $1 - 1 = 0$ . In the momentum space this occurs when one continuously changes the chemical potential from the positive to the negative value: at  $\mu < 0$  there is no vortex loop in momentum space and the

ground state (vacuum) is fully gapped. The point  $\mu = 0$  marks the quantum phase transition – the Lifshitz transition – at which the topology of the energy spectrum changes. At this transition the symmetry of the ground state does not change. Similar Lifshitz transition from the fully gapped state to the state with the Fermi surface may occur in superfluids and superconductors when the superfluid velocity crosses the Landau velocity: the symmetry of the order parameter does not change across such a quantum phase transition (see Fig. 26.1 in [6]; on other examples of the Fermi surface in superfluid/superconducting states in condensed matter and quark matter see [24]). In the non-superconducting states, the transition from the gapless to gapped state is the metal-insulator transition. The Mott transition also belongs to this class. The other types of the Lifshitz transition are related to reconnection of the vortex lines in momentum space, Fig. 3. The simplest example is provided by the spectrum  $E(\mathbf{p}) = p_x^2 - p_y^2 - \mu$ , where the reconnection quantum transition occurs at  $\mu = 0$ .

## 3 Fermi points

### 3.1 Fermi point as topological object

The crucial non-perturbative reconstruction of the spectrum occurs at the superfluid transition to  $^3\text{He-A}$ , where the point nodes emerge instead of the Fermi surface. Since we are only interested in effects determined by the topology and the symmetry of the fermionic Hamiltonian  $H(\mathbf{p})$  or Green's function  $G(\mathbf{p}, i\omega)$ , we do not require a special form of the Green's function and can choose the simplest one with the required topology and symmetry. First, consider the Bogoliubov–Nambu Hamiltonian which qualitatively describes fermionic quasiparticles in the axial state of  $p$ -wave pairing. This Hamiltonian can be applied to superfluid  $^3\text{He-A}$  [4] and also to the  $p$ -wave BCS state of ultracold Fermi gas:

$$\begin{aligned}
H &= \begin{pmatrix} p^2/2m - \mu & c_\perp \mathbf{p} \cdot (\hat{\mathbf{e}}_1 + i \hat{\mathbf{e}}_2) \\ c_\perp \mathbf{p} \cdot (\hat{\mathbf{e}}_1 - i \hat{\mathbf{e}}_2) & -p^2/2m + \mu \end{pmatrix} \\
&= \tau_3(p^2/2m - \mu) + c_\perp \mathbf{p} \cdot (\tau_1 \hat{\mathbf{e}}_1 - \tau_2 \hat{\mathbf{e}}_2),
\end{aligned} \tag{3}$$

where  $\tau_1$ ,  $\tau_2$  and  $\tau_3$  are  $2 \times 2$  Pauli matrices in Bogoliubov–Nambu particle-hole space, and we neglect the spin structure which is irrelevant for consid-

eration. The orthonormal triad  $(\hat{\mathbf{e}}_1, \hat{\mathbf{e}}_2, \hat{\mathbf{l}} \equiv \hat{\mathbf{e}}_1 \times \hat{\mathbf{e}}_2)$  characterizes the order parameter in the axial state of triplet superfluid. The unit vector  $\hat{\mathbf{l}}$  corresponds to the direction of the orbital momentum of the Cooper pair (or the diatomic molecule in case of BEC); and  $c_\perp$  is the speed of the quasiparticles if they propagate in the plane perpendicular to  $\hat{\mathbf{l}}$ .

The energy spectrum of these Bogoliubov–Nambu fermions is

$$E^2(\mathbf{p}) = \left( \frac{p^2}{2m} - \mu \right)^2 + c_\perp^2 (\mathbf{p} \times \hat{\mathbf{l}})^2. \quad (4)$$

In the BCS regime occuring for positive chemical potential  $\mu > 0$ , there are two Fermi points in 3D momentum space with  $E(\mathbf{p}) = 0$ . For the energy spectrum (4), the Fermi points are  $\mathbf{p}_1 = p_F \hat{\mathbf{l}}$  and  $\mathbf{p}_2 = -p_F \hat{\mathbf{l}}$ , with Fermi momentum  $p_F = \sqrt{2m\mu}$  (Fig. 4 *right*).

For a general system, be it relativistic or nonrelativistic, the topological stability of the Fermi point is guaranteed by the nontrivial homotopy group  $\pi_2(GL(n, \mathbf{C})) = \mathbb{Z}$  which describes the mapping of a sphere  $S^2$  embracing the point node to the space of non-degenerate complex matrices [7]. This is the group of integers. The integer valued topological invariant (winding number) can be written in terms of the fermionic propagator  $G^{-1}(i\omega, \mathbf{p}) = i\omega - H(\mathbf{p})$  as a surface integral in the 4D frequency-momentum space  $p_\mu = (\omega, \mathbf{p})$ : [6]

$$N_3 \equiv \frac{1}{24\pi^2} \epsilon_{\mu\nu\rho\sigma} \text{tr} \oint_{\Sigma_a} dS^\sigma G \frac{\partial}{\partial p_\mu} G^{-1} G \frac{\partial}{\partial p_\nu} G^{-1} G \frac{\partial}{\partial p_\rho} G^{-1}. \quad (5)$$

Here  $\Sigma_a$  is a three-dimensional surface around the isolated Fermi point  $p_{\mu a} = (0, \mathbf{p}_a)$  and ‘tr’ stands for the trace over the relevant spin and/or band indices.

For the case considered, the trace in Eq. (5) is over the Bogoliubov–Nambu spin and the two Fermi points  $\mathbf{p}_1$  and  $\mathbf{p}_2$  have nonzero topological charges  $N_3 = +1$  and  $N_3 = -1$  (Fig. 4 *right*). Close to any of the Fermi points the energy spectrum of fermionic quasiparticles acquires the relativistic form. In particular, the spectrum in Eq.(4) becomes [6]:

$$E^2(\mathbf{p}) = g^{ik} (p_i - eA_i)(p_k - eA_k), \quad (6)$$

where the analog gauge field is  $\mathbf{A} = p_F \hat{\mathbf{l}}$ , the “electric charge” is either  $e = +1$  or  $e = -1$  depending on the Fermi point, and  $g^{ik} = \text{diag}(c_\perp^2, c_\perp^2, c_\parallel^2 = p_F^2/m^2)$ . The density of states in this gapless regime is given by  $\nu(E) \propto E^2$ .

### 3.2 Quantum phase transition in BCS–BEC crossover region

Let us consider several examples of quantum phase transition governed by the momentum-space topology of gap nodes, between a fully-gapped vacuum state and a vacuum state with topologically-protected point nodes. In the context of condensed-matter physics, such a quantum phase transition may occur in a system of ultracold fermionic atoms in the region of the BEC–BCS crossover, provided Cooper pairing occurs in the non- $s$ -wave channel. For elementary particle physics, such transitions are related to CPT violation, neutrino oscillations, and other phenomena [16].

Let us start with the topological quantum phase transition involving topologically stable Fermi points [14, 15]. Let us consider what happens with the Fermi points in Eq. (4), when one varies the chemical potential  $\mu$ . For  $\mu < 0$ , Fermi points are absent and the spectrum is fully-gapped (Fig. 4). In this topologically-stable fully-gapped vacuum, the density of states is drastically different from that in the topologically-stable gapless regime:  $\nu(E) = 0$  for  $E < |\mu|$ . This demonstrates that the quantum phase transition considered is of purely topological origin. The transition occurs at  $\mu = 0$ , when two Fermi points with  $N_3 = +1$  and  $N_3 = -1$  merge and form one topologically-trivial Fermi point with  $N_3 = 0$ , which disappears at  $\mu > 0$ . The intermediate state at  $\mu = 0$  is marginal: the momentum-space topology is trivial ( $N_3 = 0$ ) and cannot protect the vacuum against decay into one of the two topologically-stable vacua unless there is a special symmetry which stabilizes the marginal node. As we shall see in the next section, the latter takes place in the Standard Model where the Fermi points are marginal.

### 3.3 Quantum phase transition in Standard Model

The vacuum of the Standard Model above the electroweak transition is marginal: there is a multiply degenerate Fermi point  $\mathbf{p} = 0$  with the total topological charge  $N_3 = 0$ . It is therefore the intermediate state between two topologically-stable vacua; (i) the fully-gapped vacuum; and (ii) the vacuum with topologically-nontrivial Fermi points. In the Standard Model, this marginal Fermi point is protected by symmetries, namely the continuous electroweak  $U(1) \times SU(2)$  symmetry (or the discrete symmetry discussed in Sec. 12.3.2 of Ref.[6]) and the CPT symmetry. Marginal gapless fermions emerg-



ing in spin systems were discussed in [25]. These massless Dirac fermions protected by symmetry differ from the chiral fermions of the Standard Model. The latter cannot be represented in terms of massless Dirac fermions, since there is no symmetry between left and right fermions in Standard Model.

Explicit violation or spontaneous breaking of electroweak or CPT symmetry transforms the marginal vacuum of the Standard Model into one of the two topologically-stable vacua [Fig. 5 *top*]. If, for example, the electroweak symmetry is broken, the marginal Fermi point disappears and the fermions become massive. This is known to happen below the symmetry breaking electroweak transition caused by Higgs mechanism where quarks and charged leptons acquire the Dirac masses. If, on the other hand, the CPT symmetry is violated, the marginal Fermi point splits into topologically-stable Fermi points which protect chiral fermions. One can speculate that in the Standard Model the latter happens with the electrically neutral leptons, the neutrinos [16, 27].

Let us consider this scenario on a simple example of a marginal Fermi point describing a *single* pair of relativistic chiral fermions, that is, one right-handed fermion and one left-handed fermion. These are Weyl fermions with Hamiltonians  $H_{\text{right}} = \boldsymbol{\sigma} \cdot \mathbf{p}$  and  $H_{\text{left}} = -\boldsymbol{\sigma} \cdot \mathbf{p}$ , where  $\boldsymbol{\sigma}$  denotes the triplet of spin Pauli matrices. Each of these Hamiltonians has a topologically-stable Fermi point  $\mathbf{p} = 0$ . The corresponding inverse Green's functions are given by

$$\begin{aligned} G_{\text{right}}^{-1}(i\omega, \mathbf{p}) &= i\omega - \boldsymbol{\sigma} \cdot \mathbf{p} , \\ G_{\text{left}}^{-1}(i\omega, \mathbf{p}) &= i\omega + \boldsymbol{\sigma} \cdot \mathbf{p} . \end{aligned} \tag{7}$$

The positions of the Fermi points coincide,  $\mathbf{p}_1 = \mathbf{p}_2 = 0$ , but their topological charges (5) are different. For this simple case, the topological charge equals the chirality of the fermions,  $N_3 = C_a$  (i.e.,  $N_3 = +1$  for the right-handed fermion and  $N_3 = -1$  for the left-handed one). The total topological charge of the Fermi point  $\mathbf{p} = 0$  is therefore zero.

The splitting of this marginal Fermi point can be described by the Hamiltonians  $H_{\text{right}} = \boldsymbol{\sigma} \cdot (\mathbf{p} - \mathbf{p}_1)$  and  $H_{\text{left}} = -\boldsymbol{\sigma} \cdot (\mathbf{p} - \mathbf{p}_2)$ , with  $\mathbf{p}_1 = -\mathbf{p}_2 \equiv \mathbf{b}$  from momentum conservation. The real vector  $\mathbf{b}$  is assumed to be odd under CPT, which introduces CPT violation into the physics. The  $4 \times 4$  matrix of

the combined Green's function has the form

$$G^{-1}(i\omega, \mathbf{p}) = \begin{pmatrix} i\omega - \boldsymbol{\sigma} \cdot (\mathbf{p} - \mathbf{b}) & 0 \\ 0 & i\omega + \boldsymbol{\sigma} \cdot (\mathbf{p} + \mathbf{b}) \end{pmatrix}. \quad (8)$$

Equation (5) shows that  $\mathbf{p}_1 = \mathbf{b}$  is the Fermi point with topological charge  $N_3 = +1$  and  $\mathbf{p}_2 = -\mathbf{b}$  the Fermi point with topological charge  $N_3 = -1$ .

Let us now consider the more general situation with both the electroweak and CPT symmetries broken. The Hamiltonian has then an additional mass term,

$$H = \begin{pmatrix} \boldsymbol{\sigma} \cdot (\mathbf{p} - \mathbf{b}) & M \\ M & -\boldsymbol{\sigma} \cdot (\mathbf{p} + \mathbf{b}) \end{pmatrix}. \quad (9)$$

The energy spectrum of Hamiltonian (9) is

$$E_{\pm}^2(\mathbf{p}) = M^2 + |\mathbf{p}|^2 + b^2 \pm 2b \sqrt{M^2 + (\mathbf{p} \cdot \hat{\mathbf{b}})^2}, \quad (10)$$

with  $\hat{\mathbf{b}} \equiv \mathbf{b}/|\mathbf{b}|$  and  $b \equiv |\mathbf{b}|$ .

Allowing for a variable parameter  $b$ , one finds a quantum phase transition at  $b = M$  between fully-gapped vacua for  $b < M$  and vacua with two isolated Fermi points for  $b > M$  [Fig. 5 *bottom*]. These Fermi points are situated at

$$\begin{aligned} \mathbf{p}_1 &= +\hat{\mathbf{b}} \sqrt{b^2 - M^2}, \\ \mathbf{p}_2 &= -\hat{\mathbf{b}} \sqrt{b^2 - M^2}. \end{aligned} \quad (11)$$

Equation (5), now with a trace over the indices of the  $4 \times 4$  Dirac matrices, shows that the Fermi point at  $\mathbf{p}_1$  has topological charge  $N_3 = +1$  and thus the right-handed chiral fermions live in the vicinity of this point. Near the Fermi point at  $\mathbf{p}_2$  with the charge  $N_3 = -1$ , the left-handed fermions live. The magnitude of the splitting of the two Fermi points is given by  $2\sqrt{b^2 - M^2}$ . At the quantum phase transition  $b = M$ , the Fermi points with opposite charge annihilate each other and form a marginal Fermi point  $\mathbf{p}_0 = 0$ . The momentum-space topology of this marginal Fermi point is trivial (topological invariant  $N_3 = +1 - 1 = 0$ ).

### 3.4 Transition in BCS–BEC crossover region with multiple nodes

The full Standard Model contains 16 chiral fermions per family and a quantum phase transition can be characterized by the appearance and splitting

of multiple marginal Fermi points. For systems of cold atoms, an example is provided by another spin-triplet  $p$ -wave state, the so-called  $\alpha$ -phase. The Bogoliubov-Nambu Hamiltonian which qualitatively describes fermionic quasiparticles in the  $\alpha$ -state is given by [3, 4]:

$$H = \begin{pmatrix} p^2/2m - \mu & (\boldsymbol{\Sigma} \cdot \mathbf{p}) c_{\perp}/\sqrt{3} \\ (\boldsymbol{\Sigma} \cdot \mathbf{p})^{\dagger} c_{\perp}/\sqrt{3} & -p^2/2m + \mu \end{pmatrix}, \quad (12)$$

with  $\boldsymbol{\Sigma} \cdot \mathbf{p} \equiv \sigma_x p_x + \exp(2\pi i/3) \sigma_y p_y + \exp(-2\pi i/3) \sigma_z p_z$ .

On the BEC side ( $\mu < 0$ ), fermions are again fully-gapped, while on the BCS side ( $\mu > 0$ ), there are four pairs of topologically protected Fermi points with charges  $N_3 = \pm 1$ , situated at the vertices of a cube in momentum space [3] (Fig. 6). The fermionic excitations in the vicinity of these points are left- and right-handed Weyl fermions.

Since the quantum phase transition between the BEC and BCS regimes of ultracold fermionic atoms and the quantum phase transition for Dirac fermions with CPT violation are described by the same momentum-space topology, we can expect common properties. An example of such a common property would be the axial or chiral anomaly. For quantum anomalies in (3+1)-dimensional systems with Fermi points and their reduction to (2+1)-dimensional systems, see, e.g., Ref. [6] and references therein.

## 4 Fermi lines

### 4.1 Fermi line as topological object

In general the zeroes of co-dimension 2 (nodal lines in 3D momentum space or point nodes in 2D momentum space) do not have the topological stability. However, if the Hamiltonian is restricted by some symmetry, the topological stability of these nodes is possible. The nodal lines do not appear in spin-triplet superconductors, but they may exist in spin-singlet superconductors [3, 26]. The analysis of topological stability of nodal lines in systems with real fermions was done by Horava [7].

### 4.2 Single band case

An example of point nodes in 2D momentum space is provided by the layered quasi-2D high- $T_c$  superconductor. In the simplest form, omitting the

mass and the amplitude of the order parameter, the 2D Bogoliubov-Nambu Hamiltonian is

$$H = \tau_3 \left( \frac{p_x^2 + p_y^2}{2m} - \mu \right) + a\tau_1(p_x^2 - \lambda p_y^2) . \quad (13)$$

In case of tetragonal crystal symmetry one has  $\lambda = 1$ , but in a more general case  $\lambda \neq 1$  and the order parameter represents the combination of  $d$ -wave ( $p_x^2 - p_y^2$ ) and  $s$ -wave ( $p_x^2 + p_y^2$ ) components. For example, experiments in high- $T_c$  cuprate  $\text{YBa}_2\text{Cu}_3\text{O}_7$  suggest  $\lambda \sim 0.7$  in this compound [22].

At  $\mu > 0$  and  $\lambda > 0$ , the energy spectrum contains 4 point nodes in 2D momentum space (or four Fermi-lines in the 3D momentum space):

$$p_x^a = \pm p_F \sqrt{\frac{\lambda}{1 + \lambda}} , \quad p_y^a = \pm p_F \sqrt{\frac{1}{1 + \lambda}} , \quad p_F^2 = 2\mu . \quad (14)$$

The problem is whether these nodes survive or not if we extend Eq.(13) to the more general Hamiltonian obeying the same symmetry. The important property of this Hamiltonian is that, as distinct from the Hamiltonian (3), it obeys the time reversal symmetry which prohibits the imaginary  $\tau_2$ -term. In the spin singlet states the Hamiltonian obeying the time reversal symmetry must satisfy the equation  $H^*(-\mathbf{p}) = H(\mathbf{p})$ . The general form of the  $2 \times 2$  Bogoliubov-Nambu spin-singlet Hamiltonian satisfying this equation can be expressed in terms of the 2D vector  $\mathbf{m}(\mathbf{p}) = (m_x(\mathbf{p}), m_y(\mathbf{p}))$ :

$$H = \tau_3 m_x(\mathbf{p}) + \tau_1 m_y(\mathbf{p}) . \quad (15)$$

Using this vector one can construct the integer valued topological invariant – the contour integral around the point node in 2D momentum space or around the nodal line in 3D momentum space:

$$N_2 = \frac{1}{2\pi} \oint dl \, \hat{\mathbf{z}} \cdot \left( \hat{\mathbf{m}} \times \frac{d\hat{\mathbf{m}}}{dl} \right) , \quad (16)$$

where  $\hat{\mathbf{m}} \equiv \mathbf{m}/|\mathbf{m}|$ . This is the winding number of the plane vector  $\mathbf{m}(\mathbf{p})$  around a vortex line in 3D momentum space or around a point vortex in 2D momentum space. The winding number is robust to any change of the Hamiltonian respecting the time reversal symmetry, and this is the reason why the node is stable.

All four nodes in the above example of Eq.(13) are topologically stable, since nodes with equal signs ( $++$  and  $--$ ) have winding number  $N_2 = +1$ , while the other two nodes have winding number  $N_2 = -1$  (Fig. 7). To destroy the nodes one must either violate the time reversal symmetry or to deform the order parameter in such a way that the nodes merge and then annihilate each other forming the fully gapped state. In the latter case, at the border between the state with nodes and the fully gapped state the quantum phase transition occurs (see Sec. 4.4). This type of quantum phase transition which involves zeroes of co-dimension 2 was also discussed in Ref.[23].

### 4.3 Multi band case

We considered the simplest case of Hamiltonians represented by  $2 \times 2$  real matrices. What happens if the Hamiltonian is more general, i.e. it is represented by  $n \times n$  matrix with  $n > 2$ : the matrix may include the spin and band indices, or in case of the quasi-2D systems with several atomic layers – the index of the layer.

For the general  $n \times n$  real matrices the classification of the topologically stable nodal lines in 3D momentum space is given by the homotopy group  $\pi_1(GL(n, \mathbf{R}))$  [7]. It determines classes of mapping of a contour  $S^1$  around the nodal line (or around a point in the 2D momentum space) to the space of non-degenerate real matrices. The topology of nodes depends on  $n$ . If  $n = 2$ , the homotopy group for lines of nodes is  $\pi_1(GL(2, \mathbf{R})) = Z$ , it is the group of integers in Eq.(16) obeying the conventional summation  $1 + 1 = 2$ . However, for larger  $n \geq 3$  the homotopy group for lines of nodes is  $\pi_1(GL(n, \mathbf{R})) = Z_2$ , which means that the summation law for the nodal lines is now  $1 + 1 = 0$ , i.e. two nodes with like topological charges annihilate each other.

Let us demonstrate this summation law on the simplest but artificial example of  $4 \times 4$  matrix  $H$ . Let us start with  $2 \times 2$  real matrix  $H$  whose planar vector  $\mathbf{m}(\mathbf{p}) = \mathbf{p} = (p_x, p_y)$ :

$$H = \tau_3 p_x + \tau_1 p_y . \quad (17)$$

Here  $\tau_3$  and  $\tau_1$  are  $2 \times 2$  matrices which have nothing to do with the Bogoliubov-Nambu matrices. The node which we interested in is at  $p_x = p_y = 0$  and has the topological charge (winding number)  $N_2 = 1$ .

Let us now introduce two bands whose Hamiltonians have opposite signs:

$$H_{11} = \tau_3 p_x + \tau_1 p_y , \quad H_{22} = -\tau_3 p_x - \tau_1 p_y , \quad (18)$$

Each Hamiltonian has a node at  $p_x = p_y = 0$  with same winding number  $N_2 = 1$ , since in the second band one has  $\mathbf{m}_2(\mathbf{p}) = -\mathbf{m}_1(\mathbf{p})$ , and  $N_2(\mathbf{m}) = N_2(-\mathbf{m})$  according to Eq.(16).

The Hamiltonians (17) and (18) can be now combined in the  $4 \times 4$  Hamiltonian which is still real:

$$H = \sigma_3(\tau_3 p_x + \tau_1 p_y) , \quad (19)$$

where  $\sigma$  matrices operate in the 2-band space. The Hamiltonian (19) has two nodes: one is for projection  $\sigma_3 = 1$  and another one – for the projection  $\sigma_3 = -1$ . Their positions in momentum space coincide. Let us now add the term with  $\sigma_1$ , which mixes the two bands (the analog of the Dirac mass term):

$$H = \sigma_3(\tau_3 p_x + \tau_1 p_y) + \sigma_1 m . \quad (20)$$

The spectrum becomes fully gapped,  $E^2 = p^2 + m^2$ , i.e. the two nodes annihilate each other. Since the nodes have the same winding number  $N_2$ , this means that the summation law for these nodes of co-dimension 2 is  $1+1=0$ , and thus the nodal points in 2D systems and nodal lines in the 3D systems with  $4 \times 4$  real Hamiltonian are described by the  $Z_2$ -group.

The above example demonstrated how in the two band systems (or in the double layer systems) the interaction between the bands (layers) induces the annihilation of likewise nodes and formation of the fully gapped state. This means that in the high- $T_c$  materials with 2, 3 or 4 cuprate layers per period, the interaction between the layers can induce a small gap even in a pure  $d$ -wave state. However, this does not necessarily occur for two reasons. First, there still can be a symmetry which forbids the annihilation, say, the symmetry between the layers or the  $\tau_2$ -symmetry. If the Bogoliubov-Nambu Hamiltonian still anti-commutes with the  $\tau_2$ -matrix, there is a generalization of the integer valued invariant in Eq.(16) to the  $2n \times 2n$  Bogoliubov-Nambu real Hamiltonian (see also [23]):

$$N_2 = -\frac{1}{4\pi i} \text{tr} \oint dl \tau_2 H^{-1} \nabla_l H . \quad (21)$$

Since the summation law for this  $N_2$  charge is  $1+1=2$ , the annihilation of like nodes is impossible and gap does not appear. This shows that the stability of and the summation law for the nodal lines depend on the type of discrete symmetry which protects topological stability. The integer valued topological

invariants protected by discrete or continuous symmetry were discussed in Chapter 12 of the book [6].

Second, even if the  $\tau_2$ -symmetry (or any other relevant symmetry) does not protect from annihilation, another scenario is possible. The interaction between the bands (layers) can lead to splitting of nodes, which then will occupy different positions in momentum space and thus cannot annihilate. Which of the two scenarios occurs – gap formation and splitting of nodes – depends on the parameters of the system. Changing these parameters one can produce the topological quantum phase transition: from the fully gapped vacuum state to the vacuum state with pairs of nodes.

#### 4.4 Quantum phase transition in high- $T_c$ superconductor

Let us return to the Hamiltonian (13) and consider what happens with gap nodes when one changes the asymmetry parameter  $\lambda$ . When  $\lambda$  crosses zero there is a quantum phase transition at which nodes in the spectrum annihilate each other and then the fully gapped spectrum develops (Fig. 7).

Probably such a quantum phase transition has something to do with the unusual behavior observed in high- $T_c$  cuprate  $\text{Pr}_{2-x}\text{Ce}_x\text{CuO}_{4-\delta}$  [28]. It was found that the field dependence of electronic specific heat is linear at  $T=2\text{K}$ , which is consistent with fully gapped state, and non-linear at  $T\geq 3\text{K}$ , which is consistent with existence of point nodes in 2D momentum space. This was interpreted in terms of the conventional phase transition with the change of symmetry from  $s$ -wave to  $d$ -wave when temperature is decreased. But the behavior of the electronic specific heat is the consequence of the topology of the spectrum rather than of the symmetry. That is why it is more natural to identify the observed behavior with the quantum phase transition which is smeared due to finite temperature.

The similar quantum phase transition also occurs when  $\mu$  crosses zero. This scenario can be realized in the BEC–BCS crossover region, see [19, 20, 21].

## 5 Quantum transitions in fully gapped systems

### 5.1 Skyrmion in 2-dimensional momentum space

The fully gapped ground states (vacua) in 2D systems or in quasi-2D thin films, though they do not have zeroes in the energy spectrum, can also be topologically non-trivial. They are characterized by the invariant obtained by dimensional reduction from the topological invariant for the Fermi point in Eq.(5):

$$\tilde{N}_3 = \frac{1}{24\pi^2} e_{\mu\nu\lambda} \mathbf{tr} \int d^2p d\omega G \partial_{p_\mu} G^{-1} G \partial_{p_\nu} G^{-1} G \partial_{p_\lambda} G^{-1} . \quad (22)$$

There is no singularity in the Green's function, and thus the integral is over the entire 3-momentum space  $p_\mu = (\omega, p_x, p_y)$ . If a crystalline system is considered the integration over  $(p_x, p_y)$  is bounded by the Brillouin zone.

An example is provided by the 2D version of the Hamiltonian (3) with  $\hat{\mathbf{l}} = \hat{\mathbf{z}}$ ,  $\hat{\mathbf{e}}_1 = \hat{\mathbf{x}}$ ,  $\hat{\mathbf{e}}_2 = \hat{\mathbf{y}}$ . Since now  $p^2 = p_x^2 + p_y^2$ , the quasiparticle energy (4) becomes

$$E^2(\mathbf{p}) = \left( \frac{p_x^2 + p_y^2}{2m} - \mu \right)^2 + c^2(p_x^2 + p_y^2) . \quad (23)$$

It is nowhere zero. The Hamiltonian (3) can be written in terms of vector  $\mathbf{g}(p_x, p_y)$ :

$$\mathcal{H} = \tau_i g_i(\mathbf{p}) \quad , \quad g_3 = \frac{p_x^2 + p_y^2}{2m} - \mu \quad , \quad g_1 = cp_x \quad , \quad g_2 = -cp_y \quad . \quad (24)$$

The distribution of the unit vector  $\hat{\mathbf{g}}(p_x, p_y) = \mathbf{g}/|\mathbf{g}|$  in the momentum space has the same structure as the skyrmion in real space (see Fig. 8). The topological invariant for this momentum-space skyrmion is given by Eq.(22) which can be rewritten in terms of the unit vector  $\hat{\mathbf{g}}(p_x, p_y)$ :

$$\tilde{N}_3 = \frac{1}{4\pi} \int dp_x dp_y \hat{\mathbf{g}} \cdot \left( \frac{\partial \hat{\mathbf{g}}}{\partial p_x} \times \frac{\partial \hat{\mathbf{g}}}{\partial p_y} \right) . \quad (25)$$

Since at infinity the unit vector field  $\hat{\mathbf{g}}$  has the same value,  $\hat{\mathbf{g}}_{p \rightarrow \infty} \rightarrow (0, 0, 1)$ , the 2-momentum space  $(p_x, p_y)$  becomes isomorphic to the compact  $S^2$  sphere.



The function  $\hat{\mathbf{g}}(\mathbf{p})$  realizes the mapping of this  $S^2$  sphere to the  $S^2$  sphere of the unit vector  $\hat{\mathbf{g}}$  with winding number  $\tilde{N}_3$ .

Note that the energy spectrum in Eq.(23) experiences an analog of the Higgs phase transition at  $\mu = mc^2$ : if  $\mu < mc^2$  the quasiparticle energy has a single minimum at  $p = 0$ , while at  $\mu > mc^2$  the minimum is at the circumference with radius  $p_0 = \sqrt{2m(\mu - mc^2)}$ . There is no symmetry breaking at this transition, since the vacuum state has the same rotational symmetry above and below the transition. That is why the point  $\mu = mc^2$  marks the quantum phase transition, at which the topology of the minima of the energy spectrum changes. However, this transition does not belong to the class of transitions which we discuss in the present review, since the topological invariant  $\tilde{N}_3$  does not change across this smooth transition.

## 5.2 Intrinsic quantum Hall and spin quantum Hall effects

The topological charge  $\tilde{N}_3$  and other similar topological charges in 2+1 systems give rise to quantization of Hall and spin-Hall conductivities, which occurs without applied magnetic field (the so-called intrinsic quantum Hall and spin quantum Hall effects). There are actually 4 responses of currents to transverse forces which are quantized under appropriate conditions. These are: (i) quantized response of the mass current (or electric current in electrically charged systems) to transverse gradient of chemical potential  $\nabla\mu$  (transverse electric field  $\mathbf{E}$ ); (ii) quantized response of the mass current (electric current) to transverse gradient of magnetic field interacting with Pauli spins; (iii) quantized response of the spin current to transverse gradient of magnetic field; and (iv) quantized response of the spin current to transverse gradient of chemical potential (transverse electric field) [29]. All these can be described using the generalized Chern-Simons term [6]:

$$F_{\text{CS}}\{\mathbf{A}_Y\} = \frac{1}{16\pi} N_{IJ} e_{\mu\nu\lambda} \int d^2x dt A_\mu^I F_{\nu\lambda}^J, \quad (26)$$

where  $A_\mu^I$  is the set of the real or auxiliary (fictitious) gauge fields. In electrically neutral systems, instead of the gauge field  $A_\mu$  one introduces the auxiliary  $U(1)$  field, so that the current is given by variation of the action with respect to  $A_\mu$ :  $\delta S / \delta A_\mu = J^\mu$ . The auxiliary  $SU(2)$  gauge field  $A_\mu^i$  is

convenient for the description of the spin-Hall effect, since the variation of the action with respect to  $A_\mu^a$  gives the spin current:  $\delta S/\delta A_\mu^i = J_i^\mu$ . Some components of the field  $A_{\mu a}$  are physical, being represented by the real physical quantities which couple to the fermionic charges. Example is provided by the external magnetic field in neutral system, which play the role of  $A_0^i$  (see Sec. 21.2 in Ref. [6]). After the current is calculated the values of the auxiliary fields are fixed. For the related phenomenon of axial anomaly, different fictitious gauge fields were introduced in Ref. [30].

The important fact is that the matrix  $N_{IJ}$  of the prefactors in the Chern-Simons term is expressed in terms of the momentum-space topological invariants:

$$N_{IJ} = \frac{1}{24\pi^2} e_{\mu\nu\lambda} \text{tr} Q_I Q_J \int d^2 p d\omega G \partial_{p_\mu} G^{-1} G \partial_{p_\nu} G^{-1} G \partial_{p_\lambda} G^{-1}, \quad (27)$$

where  $Q_I$  is the fermionic charge interacting with the gauge field  $A_\mu^I$  (in case of several fermionic species,  $Q_I$  is a matrix in the space of species).

To obtain, for example, the response of the spin current  $j_z^i$  to the electric field  $E_i$ , one must consider two fermionic charges: the electric charge  $Q_1 = e$  interacting with  $U(1)$  gauge field, and the spin along  $z$  as another charge,  $Q_2 = s_z = \hbar\sigma_z/2$ , which interacts with the fictitious  $SU(2)$  field  $A_\mu^z$ . This gives the quantized spin current response to the electric field  $j_z^i = e^{ij} \sigma_{\text{spin-Hall}} E_j$ , where  $\sigma_{\text{spin-Hall}} = (e\hbar/8\pi)N$  and  $N$  is integer:

$$N = \frac{1}{24\pi^2} e_{\mu\nu\lambda} \text{tr} \sigma_z \int d^2 p d\omega G \partial_{p_\mu} G^{-1} G \partial_{p_\nu} G^{-1} G \partial_{p_\lambda} G^{-1}, \quad (28)$$

Quantization of the spin-Hall conductivity in the commensurate lattice of vortices can be found in Ref. [31].

The above consideration is applicable, when the momentum (or quasi-momentum in solids) is the well defined quantity, otherwise (for example, in the presence of impurities) one cannot construct the invariant in terms of the Green's function  $G(\mathbf{p}, \omega)$ . However, it is not excluded that in some cases the perturbative introduction of impurities does not change the prefactor  $N_{IJ}$  in the Chern-Simons term (26) and thus does not influence the quantization: this occurs if there is no spectral flow under the adiabatic introduction of impurities. In this case the quantization is determined by the reference system – the fully gapped system from which the considered system can be obtained by the continuous deformation without the spectral flow (analogous

phenomenon for the angular momentum paradox in  $^3\text{He-A}$  was discussed in [32]). The most recent review paper on the spin current can be found in [33].

### 5.3 Plateau transitions in fully gapped 2D systems

The integer topological invariant of the ground state cannot follow the continuous parameters of the system. That is why when one changes such a parameter, for example, the thickness of the film, one finds a set of quantum phase transitions between vacua with different integer values of the invariant (Fig. 9), and thus between the plateaus in Hall or spin-Hall conductivity. The abrupt change of the topological charge cannot occur adiabatically, that is why at the points of quantum transitions fermionic quasiparticles become gapless. If two vacua with different  $\tilde{N}_3$  coexist in space, the phase boundary between them contains edge states – gapless chiral  $1+1$  fermions whose number is determined by the difference of the topological charges of the two vacua,  $\tilde{N}_3^{(1)} - \tilde{N}_3^{(2)}$  (see Chapter 22 in Ref. [6]).

### 5.4 Topological quantum phase transition in 1D quantum Ising model

Example of the topological quantum phase transition in the fully gapped 1D systems is provided by the 1-dimensional quantum Ising model whose Hamiltonian is:

$$H = -J \sum_{n=1}^N \left( h \sigma_n^x + \sigma_n^z \sigma_{n+1}^z \right) , \quad (29)$$

where  $\sigma^x$  and  $\sigma^z$  are Pauli matrices, and  $h$  is the parameter describing the external magnetic field. This system can be represented in terms of fermions with the following Hamiltonian in the continuous  $N \rightarrow \infty$  limit (see Ref. [34] and references therein):

$$H = 2J (h - \cos(pa)) \tau_3 + 2J \sin(pa) \tau_1 , \quad -\frac{\pi}{a} < p < \frac{\pi}{a} . \quad (30)$$

It is periodic in  $p$ -space with period  $2\pi/a$  where  $a$  is the lattice spacing. The integer valued topological invariant here is the same as in Eq. (21) but now along the  $p$ -circumference:

$$\tilde{N}_2 = -\frac{1}{4\pi i} \text{tr} \oint dp \, \tau_2 H^{-1} \nabla_p H . \quad (31)$$

It can be represented in terms of the Green's function

$$G^{-1} = ig_z - g_x\tau_3 + g_y\tau_1 , \quad (32)$$

where for the particular case of the model (30), the components of the 3D vector  $\mathbf{g}(p, \omega)$  are:

$$g_x(p, \omega) = 2J(h - \cos(pa)) \quad , \quad g_y(p, \omega) = 2J \sin(pa) \quad , \quad g_z(p, \omega) = \omega . \quad (33)$$

Then the invariant (31) becomes:

$$\tilde{N}_2 = \frac{1}{4\pi} \int_{-\pi/a}^{\pi/a} dp \int_{-\infty}^{\infty} d\omega \quad \hat{\mathbf{g}} \cdot \left( \frac{\partial \hat{\mathbf{g}}}{\partial p} \times \frac{\partial \hat{\mathbf{g}}}{\partial \omega} \right) . \quad (34)$$

The invariant is well defined for the fully gapped states, when  $\mathbf{g} \neq 0$  and thus the unit vector  $\hat{\mathbf{g}} = \mathbf{g}/|\mathbf{g}|$  has no singularity. In the model, for  $h \neq 1$  one has:

$$\tilde{N}_2(h < 1) = 1 \quad , \quad \tilde{N}_2(h > 1) = 0 . \quad (35)$$

The state with  $\tilde{N}_2 = 1$  is the “instanton” in the  $(\omega, p)$ -space, which is similar to the skyrmion in  $(p_x, p_y)$ -space in Fig. 8. The real space-time counterpart of such instanton can be found in Refs. [35]. It describes the periodic phase slip process occurring in superfluid  $^3\text{He-A}$  [36]. In the model, the topological structure of the instanton at  $h < 1$  can be easily revealed for  $h = 0$ . Introducing “space-time” coordinates  $t = p$  and  $z = \omega/2J$  one obtains that the unit vector  $\hat{\mathbf{g}}$  precesses sweeping the whole unit sphere during one period  $\Delta t = 2\pi/a$  (Fig. 10):

$$\hat{\mathbf{g}}(z, t) = \hat{\mathbf{z}} \cos \theta(z) + \sin \theta(z) (\hat{\mathbf{x}} \cos(at) + \hat{\mathbf{y}} \sin(at)) \quad , \quad \cot \theta(z) = z . \quad (36)$$

This state can be referred to as ‘ferromagnetic’, since in terms of spins the ground state at  $h \rightarrow 0$  is the quantum superposition of two ferromagnetic states. At  $h > 1$ , i.e. in the ‘paramagnetic’ phase, the momentum-space topology is trivial,  $\tilde{N}_2(h > 1) = 0$ .

However, there is no symmetry breaking across the transition at  $h = 1$ , since the superposition of ferromagnetic states and the paramagnetic state have the same symmetry if  $h \neq 0$ . The transition at which the topological charge  $\tilde{N}_2$  of the ground state changes without symmetry breaking is the quantum phase transition. Because of the jump in  $\tilde{N}_2$ , the transition cannot

occur adiabatically. That is why the energy gap must tend to zero at the transition, in the same way as it occurs at the plateau-plateau transition in Fig. 9. In the model, the energy spectrum  $E^2(p) = g_x^2(p) + g_y^2(p) = 4J^2 \left( (h - \cos(pa))^2 + \sin^2(pa) \right)$  has a gap  $E(0) = 2J|h - 1|$  which tends to zero at  $h \rightarrow 1$ .

## 6 Conclusion

Here we discussed the quantum phase transitions which occur between the vacuum states with the same symmetry above and below the transition. Such a transition is essentially different from conventional phase transition which is accompanied by the symmetry breaking. The discussed zero temperature phase transition is not the termination point of the line of the conventional 2-nd order phase transition: it is either an isolated point  $(q_c, 0)$  in the  $(q, T)$  plane, or the termination line of the 1-st order transition. This transition is purely topological – it is accompanied by the change of the topology of fermionic Green’s function in  $\mathbf{p}$ -space without change in the vacuum symmetry. The  $\mathbf{p}$ -space topology, in turn, depends on the symmetry of the system. The interplay between symmetry and topology leads to variety of vacuum states and thus to variety of emergent physical laws at low energy, and to variety of possible quantum phase transitions. The more interesting situations are expected for spatially inhomogeneous systems, say for systems with topological defects in  $\mathbf{r}$ -space, where the  $\mathbf{p}$ -space topology, the  $\mathbf{r}$ -space topology, and symmetry are combined [37, 7].

I thank Frans Klinkhamer for collaboration and Petr Horava for e-mail correspondence. This work is supported in part by the Russian Ministry of Education and Science, through the Leading Scientific School grant #2338.2003.2, and by the European Science Foundation COSLAB Program.

## References

- [1] H. Georgi and S.L. Glashow, Unity of all elementary particle forces, Phys. Rev. Lett. **32**, 438 (1974).
- [2] H. Georgi, H.R. Quinn and S. Weinberg, Hierarchy of interactions in unified gauge theories, Phys. Rev. Lett. **33**, 451 (1974).

- [3] G.E. Volovik and L.P. Gorkov, Superconductivity classes in the heavy fermion systems, JETP **61**, 843 (1985).
- [4] D. Vollhardt and P. Wölfle, *The Superfluid Phases of Helium 3* (Taylor and Francis, London, 1990).
- [5] N.D. Mermin, The topological theory of defects in ordered media, Rev. Mod. Phys. **51**, 591 (1979).
- [6] G.E. Volovik, *The Universe in a Helium Droplet*, Clarendon Press, Oxford (2003).
- [7] P. Horava, Stability of Fermi Surfaces and K-Theory, Phys. Rev. Lett. **95**, 016405 (2005).
- [8] V.A. Khodel and V.R. Shaginyan, Superfluidity in system with fermion condensate, JETP Lett. **51**, 553–555 (1990).
- [9] G.E. Volovik, A new class of normal Fermi liquids, JETP Lett. **53**, 222–225 (1991).
- [10] V.R. Shaginyan, A.Z. Msezane and M.Ya. Amusia, Quasiparticles and order parameter near quantum phase transition in heavy fermion metals, Phys. Lett. **A 338**, 393 (2005); cond-mat/050109.
- [11] V.A.Khodel, J.W.Clark and M.V.Zverev, Thermodynamic properties of Fermi systems with flat single-particle spectra, cond-mat/0502292.
- [12] S. Sachdev, *Quantum Phase Transitions*, Cambridge University Press, Cambridge (2003).
- [13] I.M. Lifshitz, Sov. Phys. JETP **11**, 1130 (1960).
- [14] G.E. Volovik, *Exotic properties of superfluid  $^3\text{He}$* , World Scientific, Singapore-New Jersey-London-Hong Kong, 1992
- [15] F.R. Klinkhamer and G.E. Volovik, Quantum phase transition for the BEC-BCS crossover in condensed matter physics and CPT violation in elementary particle physics, JETP Lett. **80**, 343–347 (2004); cond-mat/0407597.

- [16] F.R. Klinkhamer and G.E. Volovik, Emergent CPT violation from the splitting of Fermi points, *Int. J. Mod. Phys. A* **20**, 2795–2812 (2005); hep-th/0403037.
- [17] V. Gurarie, L. Radzihovsky and A. V. Andreev, Quantum phase transitions across  $p$ -wave Feshbach resonance, *Phys. Rev. Lett.* **94**, 230403 (2005).
- [18] S.S. Botelho and C.A.R. Sa de Melo, Quantum phase transition in the BCS-to-BEC evolution of  $p$ -wave Fermi gases, *J. Low Temp. Phys.* **140**, 409 (2005), cond-mat/0504263.
- [19] S.S. Botelho and C.A.R. Sa de Melo, Lifshitz transition in  $d$ -wave superconductors, *Phys. Rev. B* **71**, 134507 (2005).
- [20] L.S. Borkowski and C.A.R. Sa de Melo, From BCS to BEC superconductivity: Spectroscopic consequences, cond-mat/9810370.
- [21] R.D. Duncan and C.A.R. Sa de Melo, Thermodynamic properties in the evolution from BCS to Bose-Einstein condensation for a  $d$ -wave superconductor at low temperatures, *Phys. Rev. B* **62**, 9675–9687 (2000).
- [22] H.J.H. Smilde, A.A. Golubov, Ariando, G. Rijnders, J.M. Dekkers, S. Harkema, D.H.A. Blank, H. Rogalla, H. Hilgenkamp, Admixtures to  $d$ -wave gap symmetry in untwinned  $\text{YBa}_2\text{Cu}_3\text{O}_7$  superconducting films measured by angle-resolved electron tunneling, cond-mat/0510694.
- [23] X.G. Wen and A. Zee, Gapless fermions and quantum order, *Phys. Rev. B* **66**, 235110 (2002).
- [24] E. Gubankova, Conditions for existence of neutral strange quark matter, hep-ph/0507291; E. Gubankova, E. Mishchenko and F. Wilczek, Gapless surfaces in anisotropic superfluids cond-mat/0411238; Breached superfluidity via  $p$ -wave coupling, *Phys. Rev. Lett.* **94**, 110402 (2005).
- [25] X.G. Wen, Origin of gauge bosons from strong quantum correlations, *Phys. Rev. Lett.* **88**, 011602 (2002).
- [26] E.I. Blount, Symmetry properties of triplet superconductors, *Phys. Rev. B* **32**, 29352944 (1985).

- [27] F.R. Klinkhamer, Lorentz-noninvariant neutrino oscillations: model and predictions, to appear in Int. J. Mod. Phys. A, hep-ph/0407200; Lorentz and CPT violation: a simple neutrino-oscillation model, Nucl. Phys. B (Proc. Suppl.) **149**, 209-211 (2005), hep-ph/0502062.
- [28] H. Balci and R.L. Greene, Temperature dependent change in the symmetry of the order parameter in an electron-doped high-temperature superconductor, cond-mat/0402263; Anomalous change in the field dependence of the electronic specific heat of an electron-doped cuprate, Phys. Rev. Lett. **93**, 067001 (2004).
- [29] G.E. Volovik, Fractional statistics and analogs of quantum Hall effect in superfluid  $^3\text{He}$  films, AIP Conference Proceedings **194** *Quantum Fluids and Solids - 1989* eds. G.G.Ihas and Y.Takano, Gainesville, Fl. 1989, 136-146.
- [30] D.T. Son and A.R. Zhitnitsky, Quantum anomalies in dense matter, Phys. Rev. **D 70**, 074018 (2004).
- [31] O. Vafek and A. Melikyan, Index theorem and quantum order of  $d$ -wave superconductors in the vortex state, cond-mat/0509258.
- [32] G.E. Volovik, Orbital momentum of vortices and textures due to spectral flow through the gap nodes: Example of the  $^3\text{He-A}$  continuous vortex, JETP Lett. **61**, 958-964 (1995).
- [33] E.I. Rashba, Spin-orbit coupling and spin transport, cond-mat/0507007.
- [34] J. Dziarmaga, Dynamics of quantum phase transition: exact solution in quantum Ising model, cond-mat/0509490.
- [35] J.R. Hook and H.E. Hall, Orbital dynamics of  $^3\text{He-A}$  in the presence of a heat flow and a magnetic field, J. Phys. C **12**, 783-800 (1979); G.E. Volovik, Phase slippage without vortices and vector **1** oscillations in  $^3\text{He-A}$ , JETP Lett. **27**, 573-576 (1978).
- [36] D.N. Paulson, M. Krusius, and J.C. Wheatley, Experiments on orbital dynamics in superfluid  $^3\text{He-A}$ , Phys. Rev. Lett. **36**, 1322-1325 (1976)



- [37] P.G. Grinevich and G.E. Volovik, Topology of gap nodes in superfluid  $^3\text{He}$ :  $\pi_4$  homotopy group for  $^3\text{He-B}$  disclination, J. Low Temp. Phys. **72**, 371–380 (1988); M.M. Salomaa and G.E. Volovik, Cosmiclike domain walls in superfluid  $^3\text{He-B}$ : Instantons and diabolical points in  $(\mathbf{k}, \mathbf{r})$  space,” Phys. Rev. **B 37**, 9298–9311 (1988); Half-solitons in superfluid  $^3\text{He-A}$ : Novel  $\pi/2$ -Quanta of phase slippage, J. Low Temp. Phys. **74**, 319–346 (1989).

example of quantum (Lifshitz) phase transition  
between the ground states with the same symmetry,  
but with different topology in momentum space

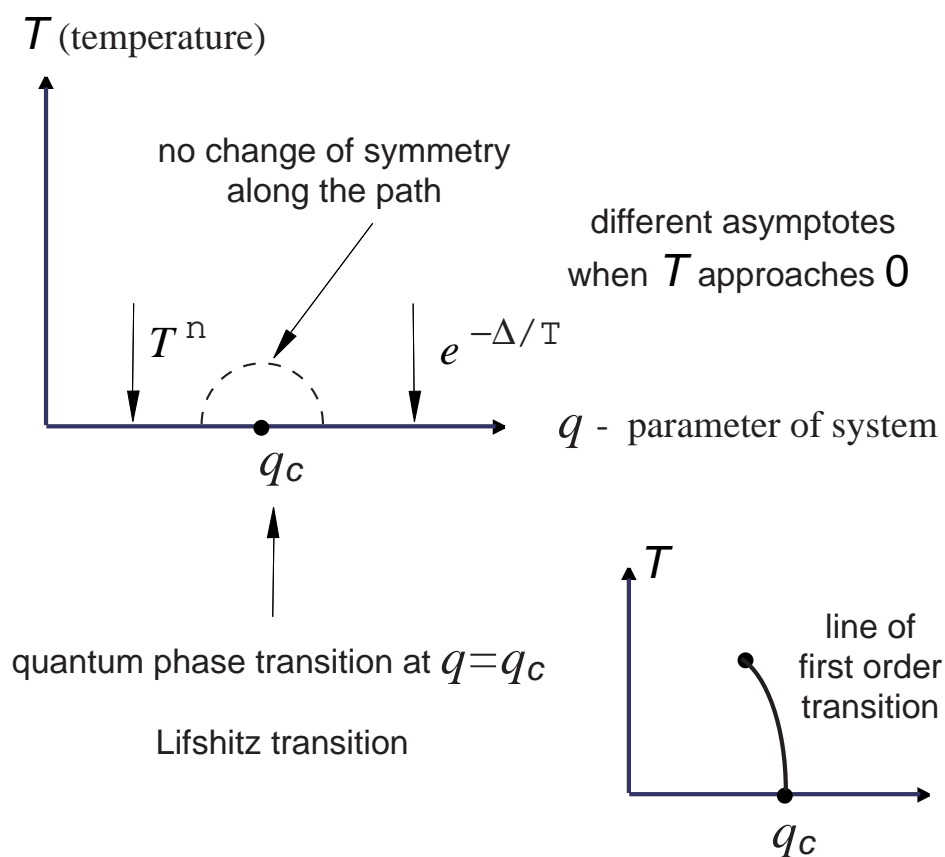


Figure 1: Quantum phase transition between two ground states with the same symmetry but of different universality class – gapless at  $q < q_c$  and fully gapped at  $q > q_c$  – as isolated point (*top*) or as the termination point of first order transition (*bottom right*).

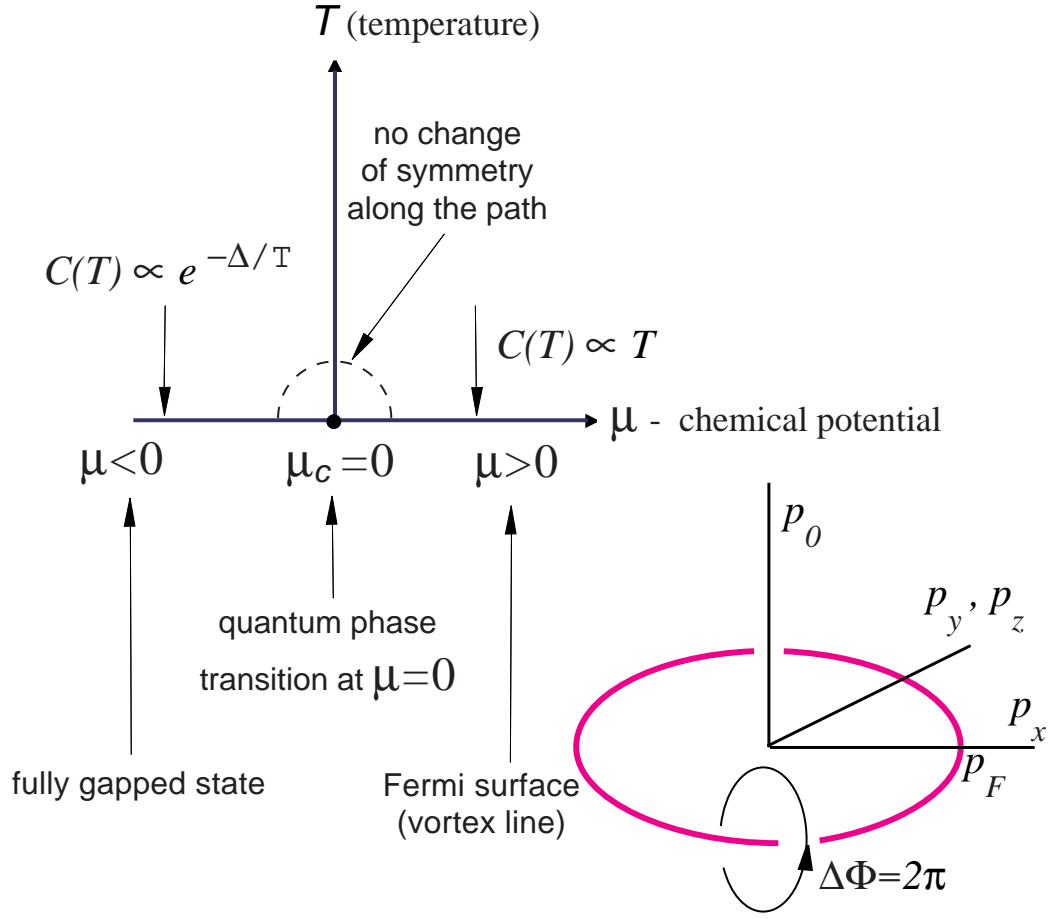


Figure 2: Fermi surface is a topological object in momentum space – a vortex loop *Bottom right*. When  $\mu$  decreases the loop shrinks and disappears at  $\mu < 0$ . The point  $\mu = T = 0$  marks the Lifshitz transition between the gapless ground state at  $\mu > 0$  to the fully gapped vacuum at  $\mu < 0$ .

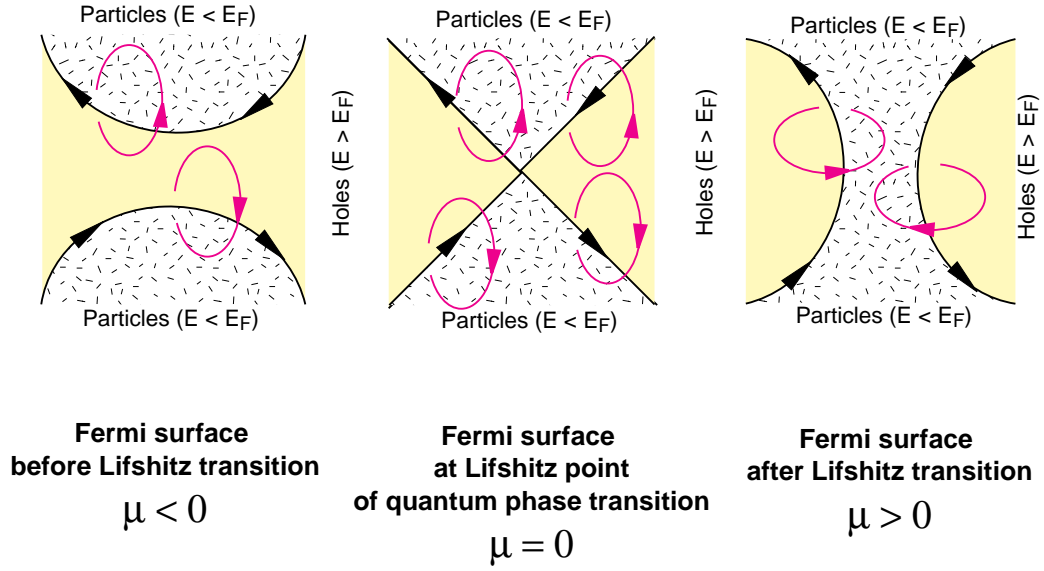


Figure 3: Lifshitz transition with change of the Fermi surface topology as reconnection of vortex lines in momentum space. Arrows show the direction of the "circulation" around and "vorticity" along the vortex line.

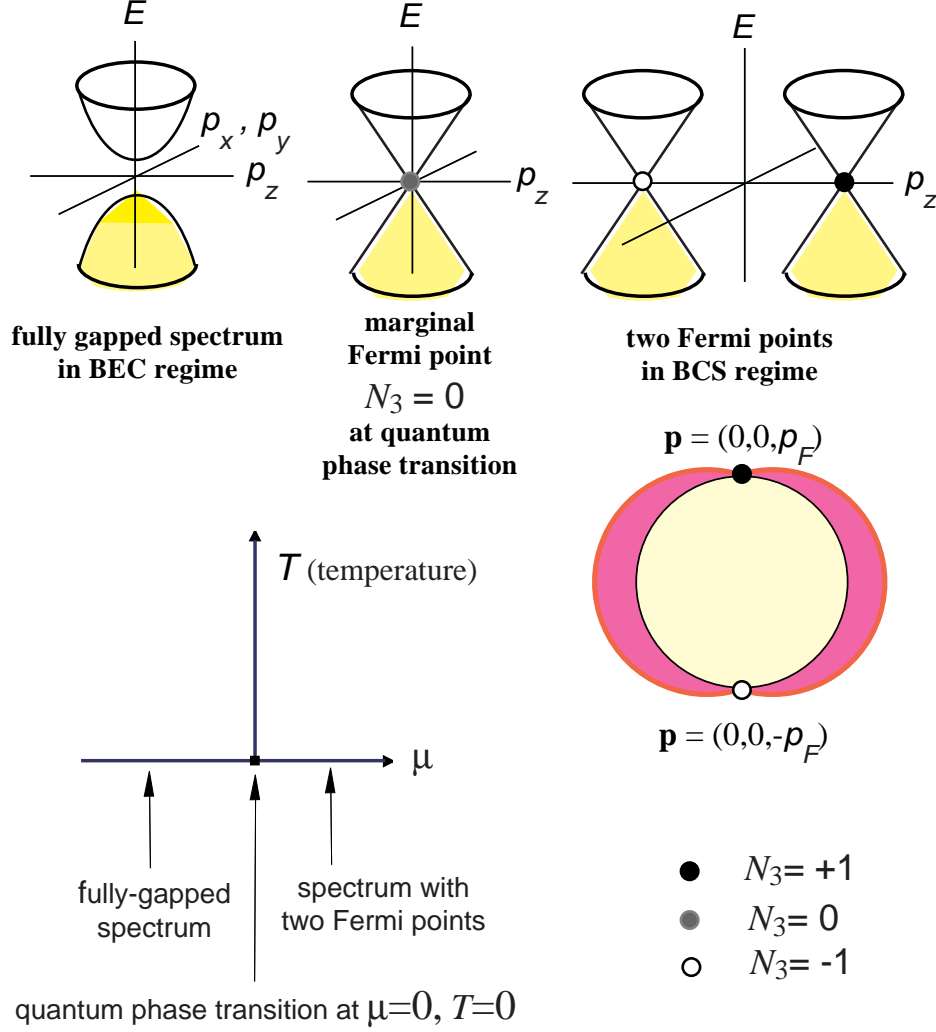


Figure 4: Quantum phase transition between two  $p$ -wave vacua with the same symmetry but of different universality class. It occurs when the chemical potential  $\mu$  in Eq.(3) crosses zero value. At  $\mu > 0$  the vacuum has two Fermi points ( $\hat{\mathbf{l}}$  is along  $z$ -axis). They annihilate each other at  $\mu = 0$ . At  $\mu < 0$  the Green function has no singularities and the quantum vacuum is fully gapped. Filled circle: gap node with winding number  $N_3 = +1$ ; open circle: gap node with  $N_3 = -1$ ; grey circle: marginal gap node with  $N_3 = 0$ .

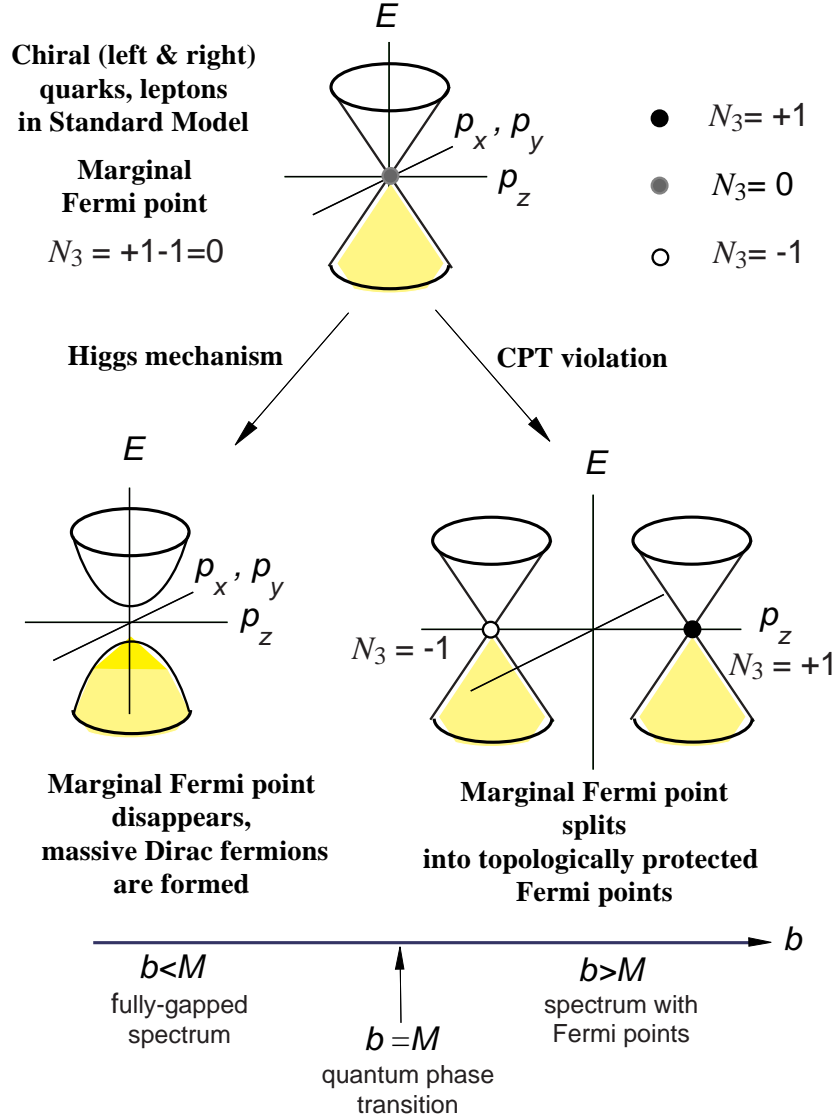


Figure 5: *top*: Two scenarios of annihilation of marginal Fermi point in Standard Model of strong and electroweak interactions. Higgs mechanism leads to Dirac mass and thus to the fully gapped vacuum, while CPT violation leads to splitting of Fermi points. *bottom*: Quantum phase transition in the model in Eq.(9) with both the Dirac mass parameter  $M$  and the CPT violating vector  $\mathbf{b}$  along  $z$ -axis ( $b \equiv |\mathbf{b}|$ ).

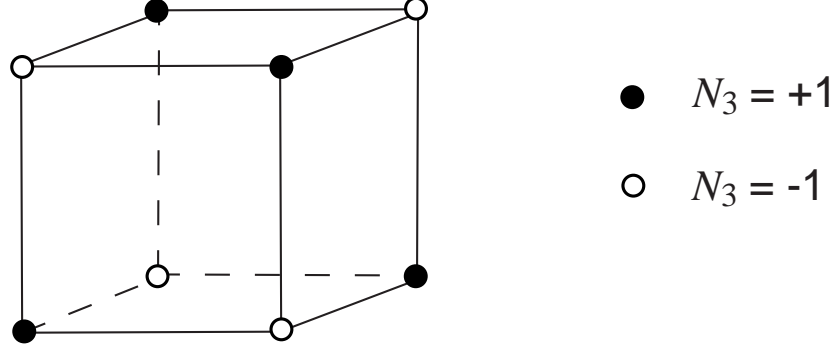


Figure 6: Fermi points in the  $\alpha$ -phase of triplet superfluid/superconductor in the BCS regime.

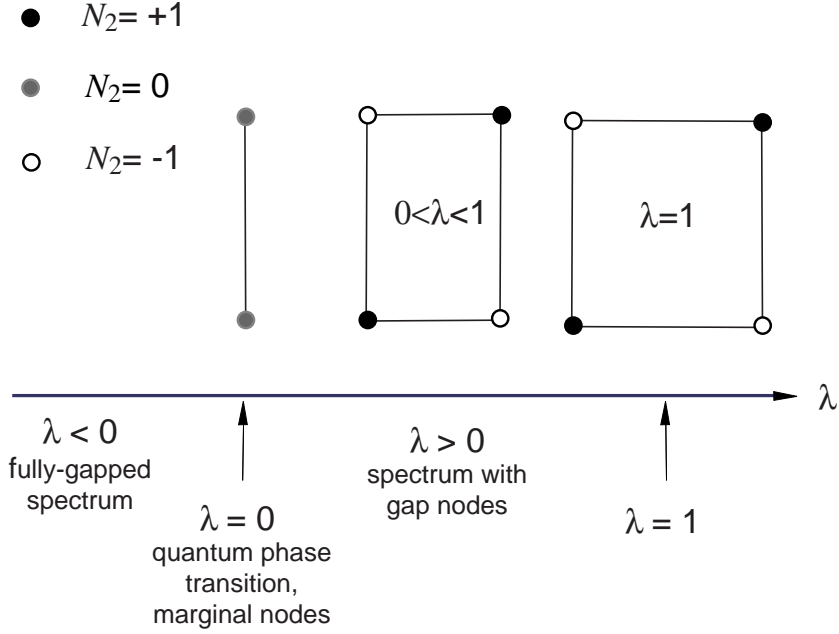


Figure 7: Quantum phase transition by change of anisotropy parameter  $\lambda$  in Eq. (13) for superconductors in  $d + s$  state. Filled circle: gap node (point node in 2D momentum space) with  $N_2 = +1$ ; open circle: gap node with  $N_2 = -1$ ; grey circle: marginal gap node with  $N_2 = 0$ .

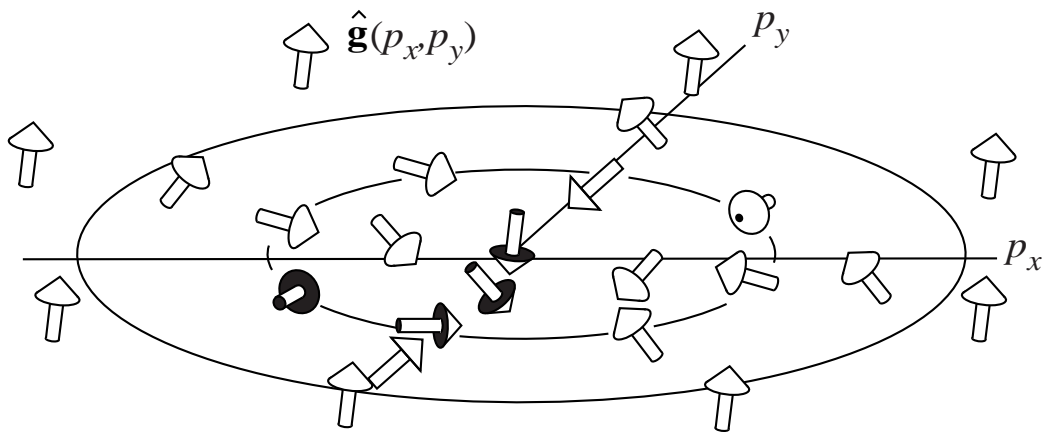


Figure 8: Skyrmion in  $\mathbf{p}$ -space with momentum space topological charge  $\tilde{N}_3 = -1$ . It describes topologically non-trivial vacua in 2+1 systems with a fully non-singular Green function.



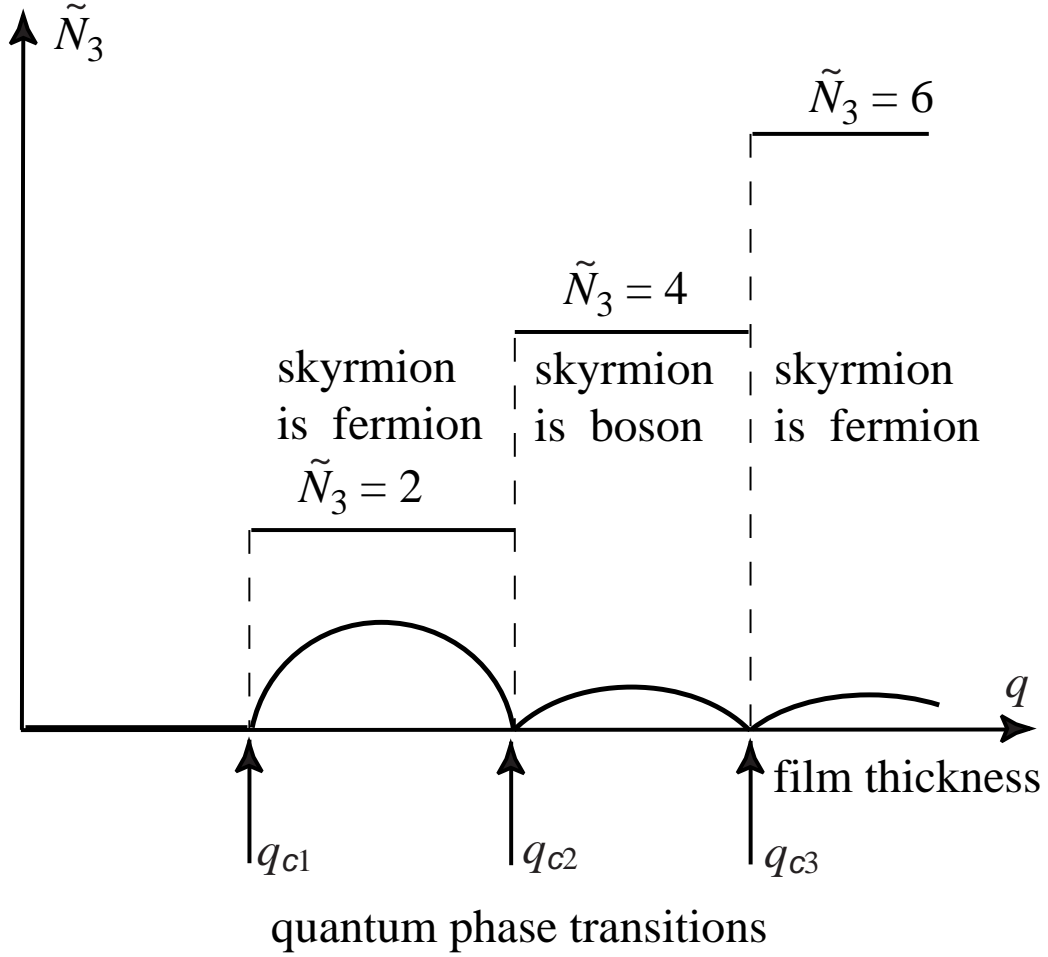


Figure 9: Quantum phase transitions occurring when one increases the thickness  $q$  of the  $^3\text{He-A}$  film. The transitions at  $q = q_{c2}$  and  $q = q_{c3}$  are plateau-plateau transitions between vacua with different values of integer topological invariant  $\tilde{N}_3$  in Eq.(22). At these transitions the quantum statistics of real-space skyrmions living in thin films changes. Thick curves show the gap in the quasiparticle energy spectrum as a function of  $q$ . The transitions at  $q = q_{c2}$  and  $q = q_{c3}$  occur between the fully gapped states, At  $q = q_{c1}$  the transition is between gapless and fully gapped states.

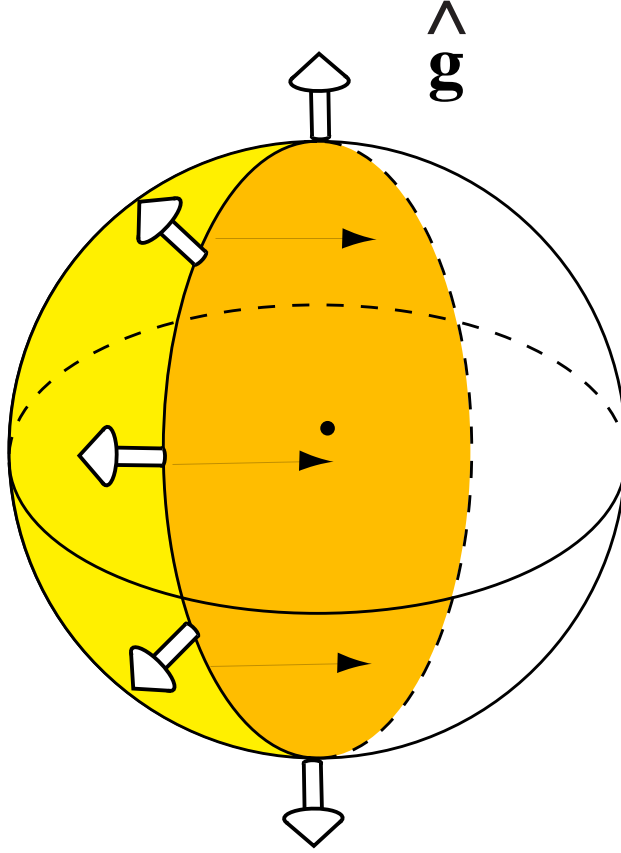


Figure 10: Illustration of the topological invariant  $\tilde{N}_2$  for ‘instanton’ in momentum space for  $h = 0$ . According to Eq.(36) one has the domain wall in  $z = \omega/2J$  space across which the direction of the vector  $\mathbf{g}$  changes from  $\hat{\mathbf{z}}$  at  $z = \infty$  to  $-\hat{\mathbf{z}}$  at  $z = -\infty$ . The structure is periodic in  $p$  and thus is precessing in ‘time’  $t = p$ . During one period of precession  $\Delta t = 2\pi/a$  the unit vector  $\hat{\mathbf{g}}(t, z)$  sweeps the whole unit sphere giving  $\tilde{N}_2 = 1$  in Eq.(34) . Black arrows show the direction of ‘precession’.